

AD-A063 728

NAVAL WEAPONS CENTER CHINA LAKE CALIF
PYROELECTRIC SURFACE ACOUSTIC WAVE SCANNED IMAGER ANALYSIS AND --ETC(U)
MAY 78 J P RAHN

F/G 17/5

UNCLASSIFIED

NWC-TM-3333

6IDEP-E107-2358

NL

1 OF 1
AD
AO 3728



END
DATE
FILMED
3-79
DDC

DDC FILE COPY ADA063728

LEVEL II

19 E107-2358

18 GIDEP

NWC Technical Memorandum 3333

9

1
SC

14 NWC-TM-3333

6 PYROELECTRIC SURFACE ACOUSTIC WAVE SCANNED
IMAGER ANALYSIS AND TESTING

by
10 J. P. Rahn
Research Department

14 May 1978

12 17 P.

16 F54584

17 WF54584601

DDC
RECEIVED
JAN 25 1979
A

Approved for public release; distribution unlimited. This is an informal report of the Naval Weapons Center and is not part of the permanent records of the Department of Defense.

62762N
138145

NAVAL WEAPONS CENTER
China Lake, California 93555

ACCESSION for	
NTIS	Write Section <input checked="" type="checkbox"/>
DDC	Buff Section <input type="checkbox"/>
UNANNOUNCED	<input type="checkbox"/>
JUSTIFICATION	
BY	
DISTRIBUTION/AVAILABILITY CODES	
Dist.	AVAIL. and/or SPECIAL
A	

79 01 23 314
403 019

mt2

26 JUL 1978

GOVERNMENT-INDUSTRY DATA EXCHANGE PROGRAM

GENERAL DOCUMENT SUMMARY SHEET

1 OF 1

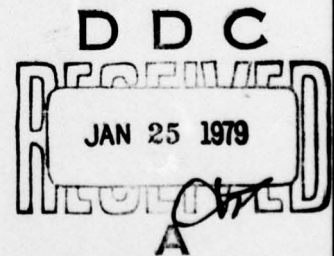
Please Type All Information - See Instructions on Reverse

1. ACCESS NUMBER E107-2358		2. COMPONENT/PART NAME PER GIDEP SUBJECT THESAURUS Optoelectronic Devices, Imaging		5. DOCUMENT ISSUE (Month/Year) May 1978
3. APPLICATION		4. MFR NOTIFICATION <input type="checkbox"/> NOTIFIED <input checked="" type="checkbox"/> NOT APPLICABLE		
6. ORIGINATOR'S DOCUMENT TITLE Pyroelectric Surface Acoustic Wave Scanned Imager Analysis & Testing			7. DOCUMENT TYPE <input checked="" type="checkbox"/> GEN RPT <input type="checkbox"/> NONSTD PART <input type="checkbox"/> SPEC	
8. ORIGINATOR'S DOCUMENT NUMBER NWC TM 3333		9. ORIGINATOR'S PART NAME/IDENTIFICATION N/A		
10. DOCUMENT (SUPERSEDES) (SUPPLEMENTS) ACCESS NO. None		11. ENVIRONMENTAL EXPOSURE CODES N/A		
12. MANUFACTURER N/A		13. MANUFACTURER PART NUMBER N/A		14. INDUSTRY/GOVERNMENT STANDARD NUMBER N/A
15. OUTLINE, TABLE OF CONTENTS, SUMMARY, OR EQUIVALENT DESCRIPTION				

This report covers information on pyroelectric imaging using SAW scanning. The results are applicable to other methods of image scanning as well.

The possibility of using surface acoustic waves (SAWs) to scan optical images on semiconductors ^{has been} was demonstrated by Quate at Stanford University in 1972. In order to do the analogous scanning of images in the infrared portion of the spectrum one has to cool the semiconductor to about 100 K. This increases initial system cost, decreases shelf life span, and requires additional servicing when operationally deployed.

One method of circumventing the cooling problem is to use the pyroelectrical effect for the infrared light sensing mechanism. When heated by incident radiation a pyroelectric develops a polarization surface charge. This polarization surface charge can exert an electric field on an adjacent semiconductor and change the charge distribution at its surface. If two SAWs in the pyroelectric interact nonlinearly with the varying surface charge in the semiconductor, then one can read out an image by observing the current versus time across the semiconductor.



79 01 23 314

16. KEY WORDS FOR INDEXING Pyroelectric Imaging; Surface Acoustic Wave Scanning; Optical Images (Doc Des--M)	
17. GIDEP REPRESENTATIVE M. H. Sloan	18. PARTICIPANT ACTIVITY AND CODE Naval Weapons Center, China Lake, CA (X7)

DD FORM 1 OCT 77 2000

REPRODUCTION OR DISPLAY OF THIS MATERIAL FOR SALES OR PUBLICITY PURPOSES IS PROHIBITED

17

FOREWORD

This report covers information on pyroelectric imaging using SAW scanning. The results are applicable to other methods of image scanning as well.

This research was performed by the Naval Weapons Center during the period October 1976 to October 1977 and was supported by the Naval Air Systems Command under Task No. WF54584601.

This report has been prepared primarily for timely presentation of information and is released at the working level.

F. C. Essig
Head, Physics Division
Research Department
1 February 1978

NWC TM 3333, published by Code 381, 25 copies.

CONTENTS

Introduction	2
Discussion	2
Appendixes:	
A. Potential Difference Between Plates of a Pyroelectric Detector Assuming Non-Uniform Illumination	9
B. Calculation of External Electric Field for a Uniformly Illuminated Pyroelectric Detector	10
C. Calculation of Ratio of Irradiance of a 1000°C Source Relative to a 1°C Above Room Temperature Source	11
D. Meaning of p: The Pyroelectric Coefficient	12
E. Calculation of Induced Detector Temperature Variation for a Given Scene Variation	13

INTRODUCTION

The possibility of using surface acoustic waves (SAWs) to scan optical images on semiconductors was demonstrated by Quate at Stanford University in 1972. In order to do the analogous scanning of images in the infrared portion of the spectrum one has to cool the semiconductor to about 100 K. This increases initial system cost, decreases shelf life span, and requires additional servicing when operationally deployed.

One method of circumventing the cooling problem is to use the pyroelectrical effect for the infrared light sensing mechanism. When heated by incident radiation a pyroelectric develops a polarization surface charge. This polarization surface charge can exert an electric field on an adjacent semiconductor and change the charge distribution at its surface. If two SAWs in the pyroelectric interact nonlinearly with the varying surface charge in the semiconductor, then one can read out an image by observing the current versus time across the semiconductor.

DISCUSSION

Several pyroelectric SAW scanned imagers (LiTaO_3 on silicon) were constructed and tested using a 1000°C blackbody source chopped at various rates. These imagers were tested with and without a germanium window to absorb the radiation of photons above the band gap of silicon. The test setup is shown in Figure 1.

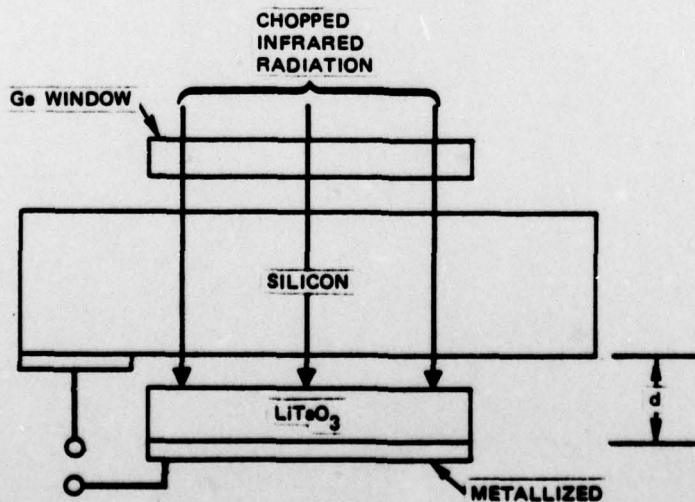


FIGURE 1. Experimental Arrangement.

For the chopping rates used, the silicon is like a perfect conductor forming the upper plate of the capacitor of plate spacing d . A potential difference between the plates is developed by heating the LiTaO_3 by infrared radiation. LiTaO_3 is a pyroelectric of moderate pyroelectric coefficient.

Radiation of wavelengths longer than $2.0 \mu\text{m}$ is transmitted by the silicon and is absorbed at the surface of the LiTaO_3 . Heat then diffuses into the LiTaO_3 , changing its temperature, and thus induces a spontaneous polarization surface charge on the LiTaO_3 .

The germanium-filtered blackbody irradiance at the device was measured to be 0.028 W/cm^2 using a Scientech thermopile. Now the black-body slide rule shows that 0.006 W/cm^2 can be absorbed in the LiTaO_3 while only 50% of this is transmitted by the silicon. This leaves 0.003 W/cm^2 absorbed at the Si-LiTaO_3 interface.

Appendix A shows that the expected potential difference between the LiTaO_3 electrode and the silicon (when this is not short-circuited) is given by

$$\Delta V = \frac{\Delta V_o A/B}{(1 + A/B)} = \frac{p \Delta H A/B}{\epsilon C_v (1 + A/B) \omega} \quad (1)$$

where

- ΔV = potential difference
- p = pyroelectric coefficient = $17 \times 10^{-5} \text{ C m}^{-2} \text{ K}^{-1}$
- ΔH = irradiance variation = 30 W m^{-2}
- A = illuminated area
- B = unilluminated area } $A/B = 0.20$
- ϵ = dielectric constant = $3.9 \times 10^{-10} \text{ F m}^{-1}$
- C_v = heat capacity = $3.2 \times 10^6 \text{ J m}^{-3} \text{ K}^{-1}$
- ω = chopper angular rate = 10 rad/s .

Thus,

$$\Delta V = 0.070 \text{ V} \quad (2)$$

Using an electrometer to avoid voltage drop across the device, this potential difference was measured to be 0.055 V . The difference is probably due to heat loss by conduction into the adjacent silicon.

When the silicon and lower electrode of the LiTaO_3 are shorted together and the device is uniformly illuminated (shown in Appendix B), the external electric field incident on the silicon is given by

$$E_{\text{ext}} = \frac{\epsilon}{\epsilon_0} \frac{\Delta V_0}{d} \quad (3)$$

where the parameters which have not been previously defined are

$$\begin{aligned} \epsilon_0 &= \text{permittivity of vacuum} = 8.9 \times 10^{-12} \text{ F m}^{-1} \\ d &= \text{thickness of LiTaO}_3 = 0.001 \text{ m.} \end{aligned}$$

The result is

$$E_{\text{ext}} = 18060 \text{ V/m} \quad (4)$$

When the semiconductor is at or near zero temperature, the charge density versus depth into the semiconductor is as shown in Figure 1, where the depth to which the charge extends is just sufficient to cancel the external field and is called the depleted depth. In this limit, the depleted depth, ΔW_0 , is related to external field by

$$\Delta W_0 = \frac{\epsilon_0 \Delta E_{\text{ext}}}{q N_D} \quad (5)$$

where

$$\begin{aligned} \Delta E_{\text{ext}} &= \text{pyroelectrically generated field} = 18060 \text{ V/m} \\ \epsilon_0 &= \text{dielectric constant of vacuum} = 9 \times 10^{-12} \text{ F m}^{-1} \\ q &= \text{electronic charge} = 1.6 \times 10^{-19} \text{ C} \\ N_D &= \text{donor density} = 10^{21} \text{ m}^{-3} \end{aligned}$$

thus

$$\Delta W_0 = 1.0 \times 10^{-9} \text{ m}$$

For finite temperatures the edge of the depleted regions is not sharp, as shown in Figure 2. The charge density in the semiconductor is given by Sze (Eq. 9.9).¹

$$\rho = -q[n_{no}(e^{\beta\psi} - 1) - p_{no}(e^{-\beta\psi} - 1)] \quad (6)$$

where ψ is a potential to be determined by the differential equation

$$E = -\frac{d\psi}{dx} = \frac{2(qn_{no}\beta)}{\beta \left(\frac{\epsilon}{\epsilon_0}\right)}^{1/2} \left[(e^{-\beta\psi} - \beta\psi - 1) + \frac{p_{no}}{n_{no}} (e^{-\beta\psi} + \beta\psi - 1) \right]^{1/2} \quad (7)$$

¹S. M. Sze. *Physics of Semiconductor Devices*. John Wiley and Sons, New York, N.Y. (1969).

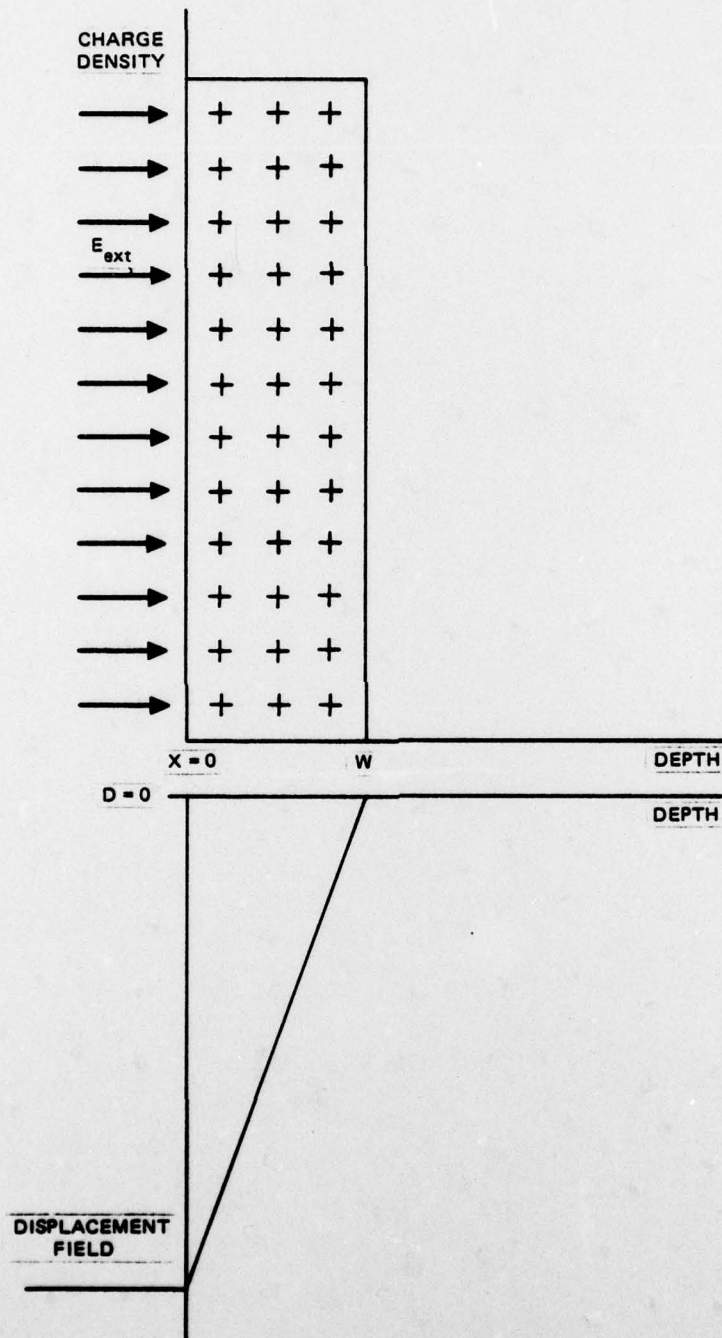


FIGURE 2. Zero Temperature Charge Density and Displacement Field.

where

$$\begin{aligned}\beta &= q/kT \\ n_{no} &= N_D \\ p_{no} n_{no} &= n_i^2 \\ k &= \text{Boltzmann's constant} \\ T &= \text{absolute temperature} \\ n_i &= \text{intrinsic charge density} = 10^{16}/\text{m}^3 \text{ at } T = 300 \text{ K}\end{aligned}$$

The term ψ at $x=0$ is determined by setting the field E equal to $E_s = E_{ext}/\epsilon_s$, where ϵ_s is the dielectric constant of the semiconductor, and iteratively solving Eq. (7) for ψ . Having obtained E_s and ψ_s , one simply solves Eq. (7) for $\psi(x)$ by iterating x in sufficiently small increments.

Having obtained $\psi(x)$ one may use Eq. (6) to obtain $\rho(x)$ versus x . This is shown in Figure 3 for several values of pyroelectric temperature. With larger external fields, such as at $E=E_4$, we obtain complete depletion (800 C/m^3) at the surface and a shape which approximates that of Figure 2 but with rounding at the edge of the depleted zone.

The important thing to note from Figure 3 is that, even with the rounding, the change in depth where half depletion occurs is approximately the same as it would be if calculated from Eq. (5) for a given external field change.

Appendix C shows that the ratio of the irradiance emanating from a chopped 1000°C source near 300 K, and relative to a source 1 K hotter than the chopper blades, is 3.46×10^4 for the $6\text{--}15 \mu\text{m}$ region to which LiTaO_3 is sensitive. This implies that the depletion depth change is $10^{-9} \text{ m} / 3.46 \times 10^4 = 2.9 \times 10^{-14} \text{ m}$ for the scene temperature variation of about 1 K. Our sensitivity expectations² using visible light on silicon are 0.01 Lux or $1.4 \times 10^{-11} \text{ W/cm}^2$ which corresponds to a depletion depth change

$$\begin{aligned}\Delta W &= \frac{H\tau}{h\nu N_d} = \frac{(1.4 \times 10^{-11} \text{ W/cm}^2)(0.033 \text{ s})}{(2.0 \times 10^{-19} \text{ J}) 10^{15}/\text{cm}^3} \\ \Delta W &= 2.3 \times 10^{-9} \text{ cm} = 2.3 \times 10^{-11} \text{ m}\end{aligned}\tag{8}$$

²H. P. Leet. "Surface Acoustic Wave IR Scan Device Technology: Image Sensor Application to Navy Air." Written for program sponsor. Copies obtainable from author at Naval Weapons Center, China Lake, California 93555.

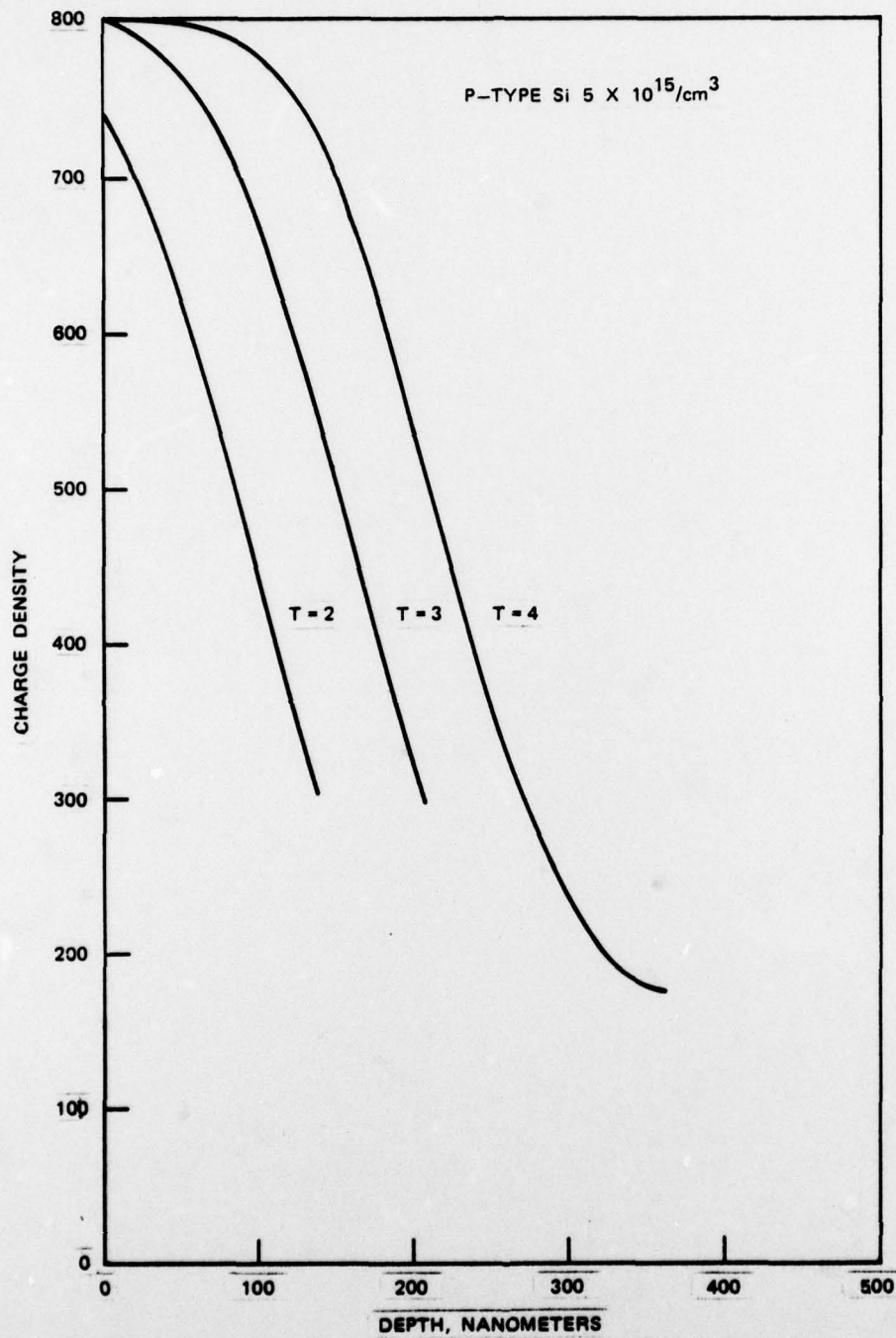


FIGURE 3. Room Temperature Charge Density.

where

$$\begin{aligned}\tau &= \text{integration time} = 0.033 \text{ s} \\ H &= \text{noise equivalent irradiance} = 1.4 \times 10^{-11} \text{ W/cm}^2 \\ h\nu &= \text{photon energy} = 2 \times 10^{-19} \text{ J} \\ N_d &= \text{donor density} = 10^{15}/\text{cm}^3\end{aligned}$$

Thus, for the pyroelectric device, the analysis shows that, even with the most sensitive configuration using silicon diodes as the semiconductor medium, we are three orders of magnitude from sensing a thermal scene and could just barely expect to sense a 1000°C scene.

The low effective quantum efficiency of a good pyroelectric was recognized more than a year ago by the author. However, there existed the possibility of some phenomenon other than depletion-depth-change-due-to-pyroelectric-charge. However, experimental investigations show no SAW attenuation or phase velocity change due to even a chopped 1000°C source focused directly onto the pyroelectric using an f/2 lens. The literature³ confuses the analysis with equations like

$$-\nabla \cdot \mathbf{E} = (\nabla \cdot \mathbf{P}_s - \rho_o)/\epsilon \quad (9)$$

where ρ_o is the free charge density, \mathbf{P}_s the spontaneous polarization, and \mathbf{E} the electric field.

The correct form is

$$-\nabla \cdot \mathbf{E} = (\nabla \cdot \mathbf{P}_s - \rho_o)/\epsilon_o \quad (10)$$

In the results of Ref. 3 this error is corrected by reinterpretation of the pyroelectric coefficient. The correct interpretation is given in Appendix D.

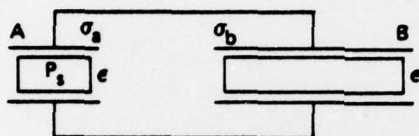
It is of interest to consider the temperature changes at the surface of LiTaO_3 when chopped, focused light of a scene 1 K hotter or colder than the chopper blades impinges on the surface. In Appendix E, this case is considered for a chopping rate of 167 Hz, which allows equilibration of the temperature variations throughout the thickness of the assumed 30- μm -thick detector [i.e., $(D/\omega)^{1/2} = 30 \mu\text{m}$ where D is the diffusion coefficient, and $\omega = 2\pi(167)$]. Note that at this chopping rate the detector temperature variations are four orders of magnitude less than the scene temperature variations.

In light of these findings, the author feels that no further effort to implement a SAW scanned pyroelectric device is warranted unless new, more favorable, geometries or materials become available.

³B. Turner and H. A. H. Boot. "The Thermo Imaging Response of a Pyroelectric Target," *Infrared Physics*, Vol. 16 (May 1975), pp. 367-374.

Appendix A

POTENTIAL DIFFERENCE BETWEEN PLATES OF A PYROELECTRIC DETECTOR
ASSUMING NON-UNIFORM ILLUMINATION



$$\sigma_a A = -\sigma_b B \text{ (charge conservation)}$$

$$V_b = V_a = \frac{\sigma_b d}{\epsilon} = -\frac{\sigma_a A d}{B \epsilon}$$

$$V_a = \frac{\sigma_a d}{\epsilon} - \Delta V_o$$

where ΔV_o is given by Eq. (19) of Ref. 3;

$$\Delta V_o = \frac{p \Delta H}{\epsilon C_v \omega}$$

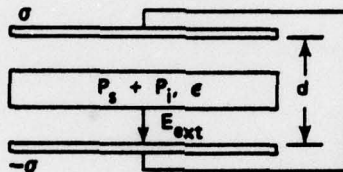
thus

$$\frac{\sigma_a d}{\epsilon} = \frac{\Delta V_o}{d(1 + A/B)}$$

then

$$V_b = \frac{A/B \Delta V_o}{(1 + A/B)}$$

Appendix B
CALCULATION OF EXTERNAL ELECTRIC FIELD FOR A
UNIFORMLY ILLUMINATED PYROELECTRIC DETECTOR



If the pyroelectric material fills the space between the plates

$$\sigma/\epsilon d - \Delta V_o = 0$$

$$\sigma = \epsilon \Delta V/d$$

$$E_{ext} = \sigma/\epsilon_o = \epsilon/\epsilon_o (\Delta V_o/d)$$

Appendix C

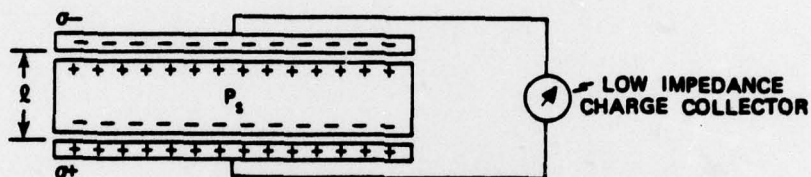
CALCULATION OF RATIO OF IRRADIANCE OF A 1000°C SOURCE
RELATIVE TO A 1°C ABOVE ROOM TEMPERATURE SOURCE

$$\frac{\Delta H (1000^\circ\text{C})}{\Delta H (1^\circ\text{C})} \quad \frac{6-15 \mu\text{m}}{6-15 \mu\text{m}}$$

$$\Delta H(301-300) = 7.4 \times 10^{-5} \text{ W/cm}^2\text{-K}$$

$$\frac{\Delta H (1000)}{\Delta H (300)} = \frac{2.56}{7.4 \times 10^{-5} \text{ W/cm}^2} = 3.46 \times 10^4$$

Appendix D
MEANING OF p:
THE PYROELECTRIC COEFFICIENT



$$P_1 + \epsilon_0 E_1 = \epsilon E_1 = \sigma$$

$$E_s = -P_s / \epsilon_0$$

$$\Delta V = (\sigma / \epsilon - P_1 / \epsilon_0) l$$

If charge flows into the charge collector such that the voltage across the device goes to zero then

$$\sigma / \epsilon = P_s / \epsilon_0 \text{ or } \sigma = P_s \epsilon / \epsilon_0 = p \Delta T$$

It is σ and not P_s which is the surface charge density per unit area generated by a 1 K change in temperature.

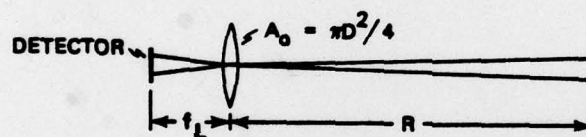
$$\text{Thus, } P_s = \epsilon_0 / \epsilon p \Delta T$$

Appendix E

CALCULATION OF INDUCED DETECTOR TEMPERATURE VARIATION
FOR A GIVEN SCENE VARIATION

Here we make a calculation of $\Delta T_D / \Delta T_s$ where ΔT_s is the scene temperature variation and ΔT_D is the detector temperature variation at its front face.

$$\frac{dP_D}{dT_s} = \frac{A_o}{R} H_s A_t = A_o H_s \Omega_t \quad (E-1)$$



where A_o is the area of the optics, H_s is the scene power output/($\text{cm}^2\text{-sr-K}$) and A_t is the area of the target. Then the irradiance variation at the detector front face is

$$\frac{\Delta H_D}{\Delta T_s} = \frac{A_o H_s}{f_L^2} \quad (E-2)$$

where f_L is the focal length of the optics and ΔH_D is the irradiance change on the detector. But $A_o/f_L^2 = \pi(\text{NA})^2$ where NA is the numerical aperture.

Thus, $H_D = (\text{NA})^2 \pi H_s$; using Holeman and Wreathall's expression for low spatial frequency and thin detectors⁴

$$\frac{\Delta T_D}{\Delta T_s} = \frac{\pi(\text{NA})^2 H_s}{C_v \omega b} \quad (E-3)$$

where

$b = 30 \mu\text{m} = 0.003 \text{ cm} = \text{detector thickness}$

$H_s = 7.4 \times 10^{-5} \text{ W/cm}^2\text{-K}$

⁴B. R. Holeman and W. M. Wreathall. "Thermal Imaging Camera Tubes with Pyroelectric Targets," *J Phys D: Appl Phys*, Vol. 4 (1971).

$$C_v = 3.2 \text{ J/cm}^3\text{-K} = \text{heat capacity/unit volume}$$

$$\omega = 2\pi(167) = \text{chopping angular frequency}$$

$$NA = 1$$

then

$$\frac{\Delta T_D}{\Delta T_s} = \frac{\pi(1)(7.4 \times 10^{-5})}{3.2(2\pi)(167)(0.003)} = 2.3 \times 10^{-5} \quad (\text{E-4})$$

One may note that the second law of thermodynamics disallows the possibility of $\Delta T_D / \Delta T_s > 1$ and we did not take into consideration heat losses due to reradiation here.